Synthesis, Structural Characterization, and Reactivity of Zirconium Complexes Containing Trimethylenemethane-Based Ligands

George Rodriguez and Guillermo C. Bazan*

Contribution from the Department of Chemistry, University of Rochester, Rochester, New York 14627-0216

Received July 24, 1996[⊗]

Abstract: General synthetic routes to zirconium metallocene-like complexes containing derivatives of the dianionic trimethylenemethane (TMM) ligand are presented. One approach consists of reacting the dilithium salts of TMM, tribenzylidenemethane (TBM), *tert*-butyltribenzylidenemethane (*t*-Bu-TBM), and dibenzylidenemethylenemethane (DBM) with either Cp^*ZrCl_3 or $CpZrCl_3(DME)$. In the case of the small TMM fragment, the product is the zwitterionic $Cp^*(TMM)Zr(\mu\text{-}Cl)_2Li(TMEDA)$ (**1**). Larger TMM derivatives give discrete salts such as $[Cp^*(TBM)ZrCl_2][Li(TMEDA)_2]$ (**2**), $[Cp(TBM)ZrCl_2][Li(TMEDA)_2]$ (**3**), $[Cp(t\text{-}Bu\text{-}TBM)ZrCl_2][Li(TMEDA)_2]$ (**4**), $[Cp^*(t\text{-}Bu\text{-}TBM)ZrCl_2][Li(TMEDA)_2]$ (**5**), and $[Cp^*(exo\text{-}endo\text{-}DBM)ZrCl_2][Li(TMEDA)_2]$ (**6**). The reaction of $TBM(LiTMEDA)_2$ with $Cp^*ZrCl_2CH_2Ph$ affords $[Cp^*(TBM)ZrCl(CH_2Ph)][Li(TMEDA)_2]$ (**9**); thus the retention of $LiCl(TMEDA)_2$ by zirconium is strong. Structural characterization of these complexes reveals crowded environments around the zirconium, especially when both TBM and Cp* are coordinated. It is also possible to take advantage of intramolecular σ-bond metathesis reactions to convert coordinated allyl ligands to TMM-related fragments. For example, $[Cp^*(TMM)Zr]_2(\mu\text{-}CH_2)$ (**10**) is derived from $Cp^*(\eta^3\text{-}CH_2C(Me)CH_2)ZrMe_2$, and $Cp^*(TBM)ZrMe(THF)$ (**12**) is from $Cp^*(PhCH_2C(CHPh)_2)ZrMe_2$ (**11**). Formation of the methylpropargyl complex $Cp^*(TBM)Zr(\eta^3\text{-}CH_2CCMe)$ (**13**) from Cp*(TBM)ZrMe(THF) and 2-butyne instead of a butenyl derivative is a consequence of steric constraints. Activation of **2**−**6** with methylaluminoxane affords homogeneous catalyst mixtures for polymerization of ethylene and 1,5-hexadiene and copolymerization of ethylene with 1-hexene. There is a strong correlation between catalyst precursor structure and reactivity. Polyethylene can also be prepared by pressurizing a vessel containing only Cp*(TBM)ZrMe(THF).

Introduction

The chemistry of electrophilic d^0 transition-metal and lanthanide metallocenes is under intense investigation. Recent progress has made a significant impact in diverse areas such as C-H activation,[1] catalytic reactions (hydrosilylation,[2] hydroamination,[3] etc.), development of reactions for organic transformations,[4] acetylene oligomerization,[5] and polymerization of olefins,[6] silanes,[7] stannanes,[8] and even primary phosphines.[9] It is abundantly clear from these studies that the choice of ligands on the coordination sphere of the metal determines stability and reactivity. Sterically demanding ancillary ligands stabilize reactive metal functionalities by preventing bimolecular deactivating reactions.[10] At the same time, ligands must be small enough to accommodate substrate approach. A fine balance therefore must be reached between catalyst longevity and reactivity. New ligands, specifically designed to stabilize early transition metals, therefore play an important role in defining future applications.

Homogeneous Ziegler−Natta polymerization is a multidisciplinary area of research which benefits considerably from advances in d^0 metallocene chemistry.[6] As a result of its commercial importance, there is considerable interest by organometallic and polymer scientists in academic and industrial laboratories in improving currently available catalysts. A principal goal of these studies is to tailor bulk properties in the final material by adjusting the ligand environment of the reactive site. Mechanistic studies have led to a better understanding of the olefin insertion transition state,[11] as well as the processes responsible for chain transfer and, consequently, control of polymer chain length.

[⊗] Abstract published in *Advance ACS Abstracts,* January 1, 1997.

(1) (a) Walsh, P. J.; Hollander, F. J.; Bergman, R. G. *Organometallics* **1993**, *12*, 3705. (b) Walsh, P. J.; Carney, M. J.; Bergman, R. G. *J. Am. Chem. Soc.* **1991**, *113*, 6343. (c) Walsh, P. J.; Hollander, F. J.; Bergman, R. G. *J. Organomet. Chem.* **1992**, *428*, 13.

(2) (a) Takahashi, T.; Hasegawa, M.; Suzuki, N.; Saburi, M.; Rousset, C. J.; Fanwick, P. E.; Negishi, E. *J. Am. Chem. Soc.* **1991**, *113*, 8564. (b) Kesti, M. R.; Waymouth, R. M. *Organometallics* **1992**, *11*, 1095.

(3) (a) Gagné, M. R.; Stern, C.; Marks, T. J. *J. Am. Chem. Soc.* **1992**, *114*, 275. (b) Li, Y. W.; Fu, P.-F.; Marks, T. J. *Organometallics* **1994**, *13*, 439.

(4) See, for example: (a) Negishi, E.-I. In *Comprehensive Organic Synthesis*; Trost, B. M.; Fleming, I., Eds.; Pergamon: Oxford, 1991; Vol. 5, Chapter 9.5, p 1163. (b) Berk, S. C.; Grossman, R. B.; Buchwald, S. L. *J. Am. Chem. Soc.* **1994**, *116*, 8593. (c) Knight, K. S.; Wang, D.; Waymouth, R. M.; Ziller, J. *J. Am. Chem. Soc.* **1994**, *116*, 1845. (d) Jensen, M.; Livinghouse, T. *J. Am. Chem. Soc.* **1989**, *111*, 4495.

(5) (a) Duchateau, R.; Van Wee, C. T.; Meetsma, A.; Teuben, J. H. *J. Am. Chem. Soc.* **1993**, *115*, 4931. (b) Heeres, H. J.; Teuben, J. H. *Organometallics* **1991**, *10*, 1980. (c) Heeres, H. J.; Heeres, A.; Teuben, J. H. *Organometallics* **1990**, *9*, 1508.

(6) For recent reviews, see: (a) Brintzinger, H. H.; Fischer, D.; Mülhaupt, R.; Rieger, B.; Waymouth, R. M. *Angew. Chem., Int. Ed. Engl.* **1995**, *34*, 1143. (b) *Ziegler Catalysts*; Fink, G., Mühaupt, R., Brintzinger, H. A., Eds.; Springer-Verlag: Berlin, 1995. (c) Thayer, A. M. *Chem. Eng. News* **1995**, *73* (37), 15. (d) Schaverien, C. J. *Adv. Organomet. Chem.* **1994**, *36*, 283. (d) Jordan, R. F. *Adv. Organomet. Chem.* **1991**, *32*, 325. (e) Marks, T. J. *Acc. Chem. Res.* **1992**, *25*, 57.

(7) (a) Harrod, J. F.; Mu, Y.; Samuel, E. *Polyhedron* **1991**, *10*, 1239. (b) Tilley, T. D. *Acc. Chem. Res.* **1993**, *26*, 22 and references therein.

(8) Imori, T.; Lu, B.; Cai, H.; Tilley, T. D. *J. Am. Chem. Soc.* **1995**, *117*, 9931.

(9) Fermin, M. C.; Stephan, D. W. *J. Am. Chem. Soc.* **1995**, *117*, 12645.

(10) Piers, W. E.; Shapiro, P. J.; Bunel, E. E.; Bercaw, J. E. *Synlett* **1990**, 74.

(11) (a) Piers, W. E.; Bercaw, J. E. *J. Am. Chem. Soc.* **1990**, *112*, 9406. (b) Grubbs, R. H.; Coates, G. W. *Acc. Chem. Res.* **1996**, *29*, 85.

S0002-7863(96)02545-0 CCC: $14.00

The majority of homogeneous Ziegler−Natta precatalysts are group 4 metallocenes containing two *monoanionic* Cp ligands (*i.e.*, Cp_2ZrCl_2 or Cp_2ZrMe_2 and structural derivatives). There is a general consensus that the species responsible for polymerization are d^0, 14-electron species (*i.e.*, $[Cp_2ZrMe]^+$) which can be generated *via* a variety of different methods. Systematic modification of the bis-Cp environment results in catalysts for stereoregular polymerizations.[6] Other ligands have found innovative applications. For example, amido ligands are smaller and less electron donating[12] than Cp. Catalysts supported by amido ligands have a special propensity to coincorporate α-olefins into growing polyethylene (PE) chains.[13]

The substitution of one Cp ligand with a *dianionic*, 6π-electron donor represents a relatively new strategy for catalyst design. Jordan originally pointed out that these substitutions decrease charge without perturbing significantly the gross molecular geometry or frontier orbitals of a bent metallocene.[14a] It is possible with these molecules to investigate how charge influences reactivity. Group 4 complexes containing the dicarbollide ($[C_2B_9H_{11}]^{2-}$),[14] aminoborollide ($[C_4H_4BN^iPr_2]^{2-}$),[15] and carboranes (*i.e.*, nido-$[2,3\text{-}R_2C_2B_4H_4]^{2-}$, where R = H or $SiMe_3$)[16] have been prepared in this context. Ligand functionalities which are nonessential for metal bonding, such as the exocyclic nitrogen in aminoborollides and the Lewis basic B−H bonds in carborane cages, have the potential of binding to the metal. In light of these complications, we sought a readily prepared, robust, and dianionic ligand free of functional groups. The use of the all-carbon trimethylenemethane (TMM) ligand is especially attractive for this purpose since modification of the framework's periphery is facile. For example, tribenzylidenemethane (TBM) can be prepared in large quantities to enhance steric protection.

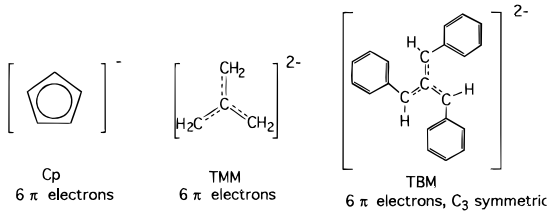

We report herein synthetic, structural, and reactivity studies of zirconium complexes containing TMM-based ligands. With these complexes we can compare the performance of *neutral* 14-electron molecules such as Cp*(TMM)ZrR (Cp* = C_5Me_5) or Cp(TBM)ZrR (R = hydride or alkyl) against the activity of well-understood metallocenes (*i.e.*, $[Cp_2ZrR]^+$) to gain insight into the effect of charge on reactivity and stability.

Scheme 1

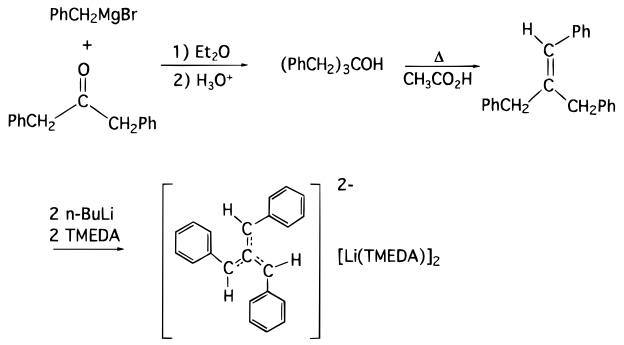

Results and Discussion

Synthetic and Structural Studies. Dianionic ligand salts are accessible by deprotonation procedures; for example, Li_2-(TMM)$(TMEDA)_2$ (TMEDA = tetramethylethylenediamine) is obtained by condensing isobutylene onto a pentane solution containing 2 equiv of *n*-butyllithium and TMEDA and collecting the resulting yellow precipitate. As is the case for all of its derivatives, Li_2(TMM)$(TMEDA)_2$ is oxygen and moisture sensitive and ignites spontaneously when exposed to air. The reaction of Li_2(TMM)$(TMEDA)_2$ with Cp^*ZrCl_3 yields Cp*-(TMM)Zr(μ-Cl)$_2$Li(TMEDA) (**1** in eq 1) as a pale yellow solid

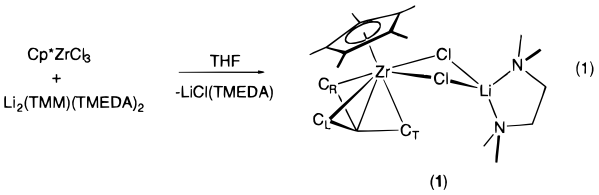

which decomposes quickly upon exposure to air. Previous work[17] has shown that the overall molecular connectivity of **1** is similar to zwitterionic yttrium and lanthanide metallocene halides (*i.e.*, $Cp^*_2Y(\mu\text{-}Cl)_2Li(EtO)_2$ or $Cp_2Lu(\mu\text{-}Cl)_2Na(DME)_2$)[18,19] and other molecules containing dianionic ligands (*i.e.*, $Cp^*(C_4H_4BN^iPr_2)Zr(\mu\text{-}Cl)_2Li(Et_2O)_2$).[15] The TMM ligand in **1** binds in a pyramidal η^4 fashion with the central carbon directed away from the metal. The Cp* ligand directs more subtle structural features. For example, the difference in Zr−methylene bond lengths (2.39(1) Å (Zr−C_L) and 2.35(1) Å (Zr−C_R) vs 2.56(1) Å (Zr−C_T)) is a clear manifestation of the strong trans effect of Cp*.

Synthesis of the larger TBM ligand begins with the reaction of $PhCH_2MgBr$ and 1,3-diphenylacetone in diethyl ether (Scheme 1).[20] The resulting magnesium alkoxide precipitate is converted to tribenzylcarbinol by aqueous workup. Subsequent dehydration in refluxing acetic acid affords 2-benzyl-1,3-diphenyl-1-propene quantitatively. Double lithiation is carried out by addition of 2 equiv of *n*-butyllithium and TMEDA to a pentane solution containing the olefin. As the reaction proceeds, the solution initially acquires an orange color which changes to deep red. Li_2(TBM)$(TMEDA)_2$ precipitates from the reaction mixture as a red solid in 60−70% overall yield. A C_3-symmetric arrangement of the three phenyl groups is confirmed

(12) (a) Shapiro, P. J.; Bunel, E.; Schaefer, W. P.; Bercaw, J. E. *Organometallics* **1990**, *9*, 867. (b) Scollard, J. D.; McConville, D. H.; Vittal, J. J. *Organometallics* **1995**, *14*, 5478.

(13) Lai, S.-Y.; Wilson, J. R.; Knight, G. W.; Stevens, J. C.; Chum, P.-W. U.S. Patent 5272236, 1993.

(14) (a) Crowther, D. J.; Baenziger, N. C.; Jordan, R. F. *J. Am. Chem. Soc.* **1991**, *113*, 1455. (b) Bazan, G. C.; Schaefer, W. P.; Bercaw, J. E. *Organometallics* **1993**, *12*, 2126. (c) Uhrhammer, R.; Crowther, D. J.; Olson, J. D.; Swenson, D. C.; Jordan, R. F. *Organometallics* **1992**, *11*, 3098. (d) Crowther, D. J.; Swenson, D. C.; Jordan, R. F. *J. Am. Chem. Soc.* **1995**, *117*, 10403.

(15) (a) Quan, R. W.; Bazan, G. C.; Kiely, A. F.; Schaeffer, W. P.; Bercaw, J. E. *J. Am. Chem. Soc.* **1994**, *116*, 4489. (b) Bazan, G. C.; Rodriguez, G. *Polyhedron* **1995**, *14*, 93. (c) Bazan, G. C.; Donnelly, S. J.; Rodriguez, G. *J. Am. Chem. Soc.* **1995**, *117*, 2671.

(16) (a) Jia, L.; Zhang, H.; Hosmane, N. S. *Organometallics* **1992**, *11*, 2957. (b) For related work, refer to: Houseknecht, K. L.; Stockman, K. E.; Sabat, M.; Finn, M. G.; Grimes, R. N. *J. Am. Chem. Soc.* **1995**, *117*, 1163.

(17) Bazan, G. C.; Rodriguez, G.; Cleary, B. P. *J. Am. Chem. Soc.* **1994**, *116*, 2177.

(18) (a) Evans, W. J.; Bole, T. J.; Ziller, J. W. *Inorg. Chem.* **1992**, *31*, 1120. (b) Coughlin, E. B.; Bercaw, J. E. *J. Am. Chem. Soc.* **1992**, *114*, 7606.

(19) (a) Watson, P. L.; Whitney, J. F.; Harlow, R. L. *Inorg. Chem.* **1981**, *20*, 3271. (b) Rausch, M. D.; Moriarty, K. J.; Atwood, J. L.; Weeks, J. A.; Hunter, W. E.; Brittain, H. G. *Organometallics* **1986**, *5*, 1281.

(20) Dieter, W.; Dietrich, H.; Clark, T.; Mahdi, W.; Kos, A. J.; Schleyer, P. v. R. *J. Am. Chem. Soc.* **1984**, *106*, 7279.

by ^{1}H NMR spectroscopy where resonances from only one type of phenyl ring are observed.

The reactivities of Li_2(TMM)(TMEDA)$_2$ and Li_2(TBM)-(TMEDA)$_2$ toward Cp*$ZrCl_3$ are different. From the slow addition of Li_2(TBM)(TMEDA)$_2$ to Cp*$ZrCl_3$ in toluene, a red product is obtained which, by NMR spectroscopy and elemental analysis, contains two TMEDA molecules per "Cp*Zr(TBM)" core. The results from an X-ray crystallographic study revealed that, unlike the zwitterionic arrangement of **1**, **2** is a discrete salt consisting of zirconate anions, [Cp*(TBM)$ZrCl_2$], accompanied by tetrahedral Li[TMEDA]$_2$ countercations (see **2** in eq 2). While rare, this structural motif has precedent in

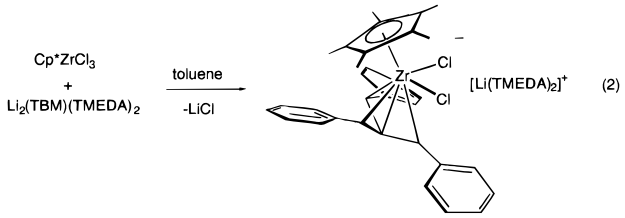

(**2**)

lanthanide chemistry.[21] Structural distortions enforced by Cp* are more pronounced in **2** than in **1**. The strong trans effect of Cp* is demonstrated by a weakened Zr−C_T interaction (see Table 1 for metrical data and nomenclature). The TBM ligand is bound in the electronically favored *syn* geometry.[22] The resulting charge and the additional steric hindrance increase the distances between Zr and the "TMM core" of TBM in **2** relative to the corresponding Zr−TMM distances in **1** (Table 1).

We have successfully coordinated TBM using other starting materials. $CpZrCl_3$(DME) reacts with Li_2(TBM)(TMEDA)$_2$ to give [Cp(TBM)$ZrCl_2$][Li(TMEDA)$_2$] (compound **3** in eq 3) in 46% yield. A crystallographic study confirms an arrangement

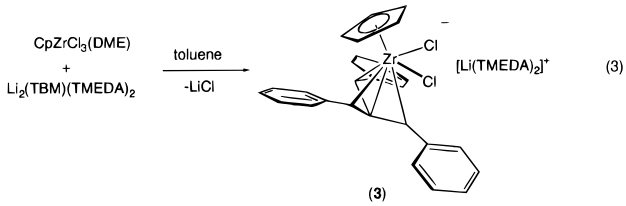

(**3**)

similar to that of **2** (see Figure 1 and Table 5 for a summary of crystallographic data). The X-ray data for this compound were of good quality; however, one of the [Li(TMEDA)$_2$] countercations was disordered, resulting in a high residual electron density around the lithium ion. The rest of the atoms were readily located and properly refined, thus providing a reliable model (see Supporting Information). Compared to **2**, the smaller Cp ligand allows the relative orientation of the phenyl groups to adopt a more pronounced propeller-like arrangement. The TBM ligand also binds more tightly. This is especially obvious in the contraction of the Zr−C_T distance, from 2.78(1) Å in **2** to 2.597(6) Å in **3**.

(21) (a) Schumann, H.; Meese-Marktscheffel, J. A.; Hahn, F. E. *J. Organomet. Chem.* **1990**, *390*, 301. (b) Kilimann, U.; Schäfer, M.; Herbst-Irmer, R.; Edelmann, F. T. *J. Organomet. Chem.* **1994**, *469*, C15. (c) Schumann, H.; Albrecht, I.; Pickardt, J.; Hahn, E. *J. Organomet. Chem.* **1984**, *276*, C5. (d) Evans, W. J.; Olofson, J. M.; Zhang, H.; Atwood, J. L. *Organometallics* **1988**, *7*, 629. (e) Schumann, H.; Albrecht, I.; Gallagher, M.; Hahn, E.; Janiak, C.; Kolax, C.; Loebel, J.; Nickel, S.; Palamidis, E. *Polyhedron* **1988**, *7*, 2307.

(22) For a discussion of *syn* vs *anti* and electronic preference for the *syn* isomer, see: Athens, S. R.; Barnes, S. G.; Green, M.; Moran, G.; Trollope, L.; Marrall, N. W.; Welch, A. J.; Shoroius, D. M. *J. Chem. Soc., Dalton Trans.* **1984**, 1157.

The sequence of steps shown in Scheme 1 is flexible, providing easy access to structurally diverse TMM-based ligands. Using 4-*tert*-butylbenzyl-MgBr instead of benzyl-MgBr allows for the synthesis of Li_2(*t*-Bu-TBM)(TMEDA)$_2$, which in turn is used to make [Cp(*t*-Bu-TBM)$ZrCl_2$][Li(TMEDA)$_2$] (**4**) and [Cp*(*t*-Bu-TBM)$ZrCl_2$][Li(TMEDA)$_2$] (**5**) from $CpZrCl_3$-(DME) and Cp*$ZrCl_3$, respectively (eq 4). The *tert*-butyl group breaks the symmetry in these molecules thereby increasing their solubility in aliphatic solvents. In fact, **4** and **5** are obtained as viscous oils which are difficult to purify and isolate in good yields.

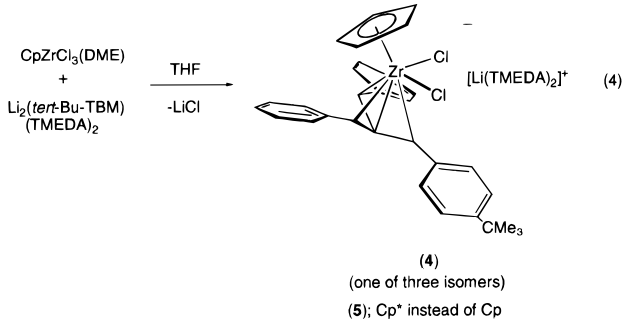

(**4**)
(one of three isomers)
(**5**); Cp* instead of Cp

Similarly, reaction of MeMgBr with 1,3-diphenylacetone provides the mixture of olefins shown in Scheme 2. After deprotonation, only one isomer of Li_2(DBM)(TMEDA)$_2$ (DBM = dibenzylidenemethylenemethane) is obtained, which readily forms [Cp*(DBM)$ZrCl_2$][Li(TMEDA)$_2$] (**6**) when reacted with Cp*$ZrCl_3$ (eq 5). A single crystal structure determination of **6**

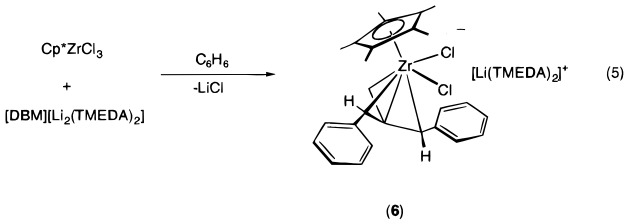

(**6**)

shows that, like **2**, it is a discrete salt, and the Cp* ligand governs most of the intramolecular distances and ligand orientations. The DBM is oriented so that one of the benzylidene arms is opposite the Cp* centroid. The smaller methylene arm is at the "back" of the molecule, away from the chlorides and closest to Cp* where steric interactions are more severe. The relative orientation of the two phenyl rings around the DBM periphery is of interest. Wilhelm demonstrated that the two phenyl rings in Li_2(DBM)(TMEDA)$_2$ exist in an *exo-exo* geometry.[23] As seen in Figure 2, the two phenyl rings of the DBM ligand in **6** lie in an *exo-endo* arrangement. Thus, **6** is best described as [Cp*(*exo-endo*-DBM)$ZrCl_2$][Li(TMEDA)$_2$]. The mechanism for how the two phenyl rings change their relative orientations is not clear at the present time.

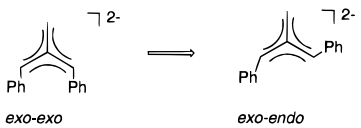

exo-exo *exo-endo*

Despite several attempts, we were not able to exchange cleanly the chloride ligands in complexes **1**, **2**, **3**, or **6**. Of all

(23) (a) Wilhelm, D.; Clark, T.; Schleyer, P. v. R.; Buckl, K.; Boche, G. *Chem. Ber.* **1983**, *116*, 1669. (b) Wilhelm, D.; Dietrich, H.; Clark, T.; Mahdi, W.; Kos, A. J.; Schleyer, P. v. R. *J. Am. Chem. Soc.* **1984**, *106*, 7279.

Table 1. Selected Bond Distances (Å) and Angles (Degrees)[a]

complex	Cl_R	Cl_L	C_I	C_T	C_R	C_L	$C_{Pcent}-Zr-C_I$
1	2.535(4)	2.545(3)	2.30(1)	2.56(1)	2.35(1)	2.39(1)	132.3(1)
2	2.498(3)	2.482(3)	2.35(1)	2.78(1)	2.45(1)	2.48(1)	135.5(2)
3	2.471(2)	2.473(2)	2.323(6)	2.597(6)	2.477(2)	2.457(7)	134.8(4)
6	2.468(7)	2.491(6)	2.32(2)	2.66(2)	2.41(2)	2.47(2)	133.5(2)
9	NA	2.459(2)	2.357(5)	2.659(6)	2.465(5)	2.476(6)	134.9(4)
13	NA	NA	2.337(4)	2.744(4)	2.397(4)	2.480(4)	134.7(4)

[a] The atom designators are defined by the following figure:

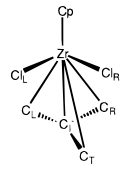

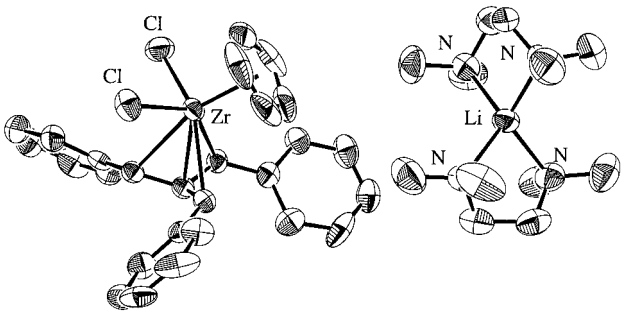

Figure 1. ORTEP diagram of **3**. Thermal ellipsoids are at 50% probability.

the alkylating agents used (LiR, R = Me, Et, CH_2SiMe_3, CH_2-Ph; MgClR, R = Me, CH_2Ph, allyl), the best result was obtained when **2** was treated with 2.5 equiv of MeLi in diethyl ether to give $[Cp^*(TBM)ZrMe_2][Li(TMEDA)_2]$ (**7** in eq 6). The low yield of this reaction (10%) and the difficulties in removing residual impurities prompted us to look at alternative strategies.

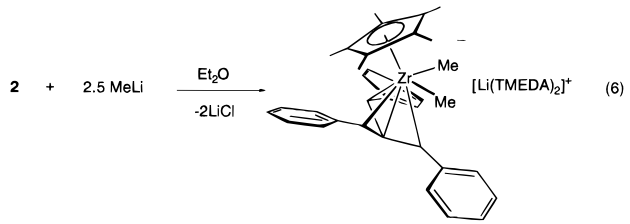

Alkylation prior to TBM coordination was considered. Both $Cp^*ZrCl_2(CH_2Ph)$[24] and $Cp^*ZrCl_2[CH(SiMe_3)_2]$ react with Li_2-$(TBM)(TMEDA)_2$ to produce $[Cp^*(TBM)ZrCl][CH(SiMe_3)_2]]$-$[Li(TMEDA)_2]$ (**8**) and $[Cp^*(TBM)ZrCl(CH_2Ph)][Li(TMEDA)_2]$ (**9**), respectively (eq 7). Removal of the second chloride was not possible using potential dehalogenating reagents such as $AlCl_3$, BCl_3, and $[Ag][BPh_4]$. The propensity of zirconium to retain the second chloride is somewhat surprising in view of the large size of the $CH(SiMe_3)_2$ fragment and the potential of the benzyl ligand to participate in multihapto bonding.[25] As shown in Figure 3, the overall molecular structure of **9** is quite similar to **2** with the benzyl group positioned to point away from Cp* and fill the cavity between two benzylidene arms of TBM.

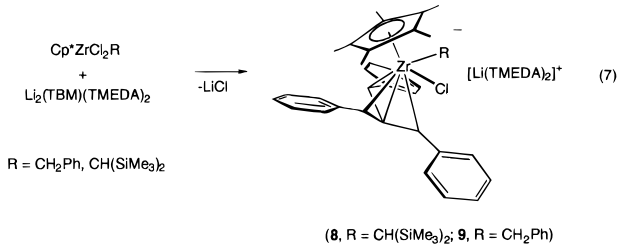

Neutral TBM and TMM Alkyl Complexes *via* σ-Bond Metathesis. The recurring alkylation problems described above prompted the search for a different approach to Cp*(TBM)-ZrR. Precedent in the literature exists for the formation of TMM by intramolecular σ-bond metathesis. Bercaw and co-workers reported the clean decomposition of $Cp^*TaMe_3(\eta^3$-CH_2-$CMeCH_2)$,[26] formed *in situ* by reaction of Cp^*TaMe_3Cl and CH_2CMeCH_2MgBr, to $Cp^*(TMM)TaMe_2$ and 1 equiv of methane. Substituting Cp^*ZrMe_2Cl for Cp^*TaMe_3Cl seemed like an obvious extension to generate the "TMM−Zr" core. Addition of $(CH_2CMeCH_2)MgBr$ to a cold solution of Cp^*ZrMe_2-Cl induced an immediate color change from yellow to orange with concomitant evolution of gas. A single product was obtained which, by ^1H NMR spectroscopy, displays one Cp* singlet and seven inequivalent hydrogens. Six of these signals are assigned by ^1H NMR COSY to a conformationally locked TMM ligand (Figure 4). The ^{13}C NMR spectrum confirms the presence of TMM with peaks at 77.3, 66.0, and 62.4 ppm for the peripheral carbons (all triplets in the ^{13}C NMR gated-decoupled spectrum) and a low-field ^{13}C signal at 180.1 ppm for the inner TMM carbon (singlet in the ^{13}C NMR gated-decoupled spectrum). Only two signals remain unaccounted for: the ^1H singlet at 4.02 ppm and the low-field ^{13}C signal at 146.5 ppm (triplet in the gated-decoupled spectrum). We propose that these resonances arise from a bridging methylene ligand, and therefore the product is $[Cp^*(TMM)Zr]_2(\mu$-$CH_2)$ (**10**), as shown in Scheme 3. The connectivity of **10** is reminiscent of that of the dicarbollide dimers $[Cp^*(C_2B_9H_{11})$-$Zr]_2(\mu$-$CH_2)$ reported by Jordan.[14a]

The formation of **10** is too quick for mechanistic investigations. However, it is likely that the initial steps involve formation of $Cp^*Zr(\eta^3$-$CH_2CMeCH_2)Me_2$ followed by intramolecular σ-bond metathesis to give short-lived [Cp*(TMM)ZrMe]. Finally, two molecules of [Cp*(TMM)ZrMe] combine to give **10** and methane. Efforts to intercept transient [Cp*(TMM)-ZrMe] using potential trapping agents such as 2-butyne or PMe_3 were unsuccessful.

A similar strategy was envisioned for preparing Cp*(TBM)-ZrMe using Cp^*ZrMe_2Cl and *endo-endo*-[Li][$PhCH_2C(CHPh)_2$].[27]

(24) Wolczanski, P. T.; Bercaw, J. E. *Organometallics* **1982**, *1*, 793.

(25) (a) Bochmann, M.; Karger, G.; Jaggar, A. J. *J. Chem. Soc., Chem. Commun.* **1990**, 1035. (b) Pellecchia, C.; Grassi, A.; Zambelli, A. *Organometallics* **1994**, *13*, 298. (c) Pellecchia, C.; Grassi, A.; Immirzi, A. *J. Am. Chem. Soc.* **1993**, *115*, 1160. (d) Pellecchia, C.; Grassi, A.; Zambelli, A. *Organometallics* **1994**, *13*, 298.

(26) Mayer, J. M.; Curtis, C. J.; Bercaw, J. E. *J. Am. Chem. Soc.* **1983**, *105*, 2651.

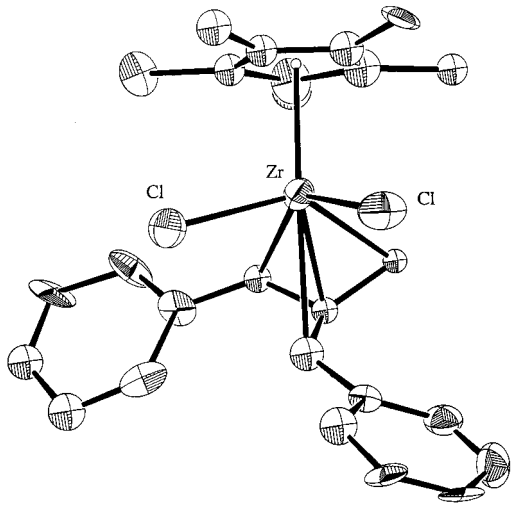

Figure 2. ORTEP diagram of **6**. The countercation is omitted for clarity. Thermal ellipsoids are drawn at the 50% probability level.

Scheme 2

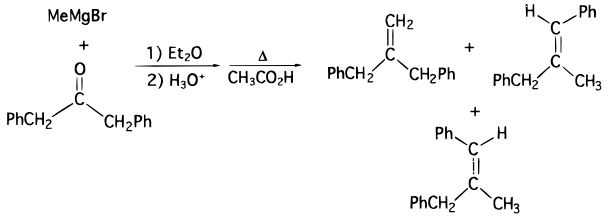

We anticipated that the large steric field of the TBM ligand would disfavor dimer formation. The first reaction proceeds cleanly to give thermally unstable $Cp^*ZrMe_2(PhCH_2C(CHPh)_2)$ (**11**). Two resonances in the ^1H NMR spectrum at 4.54 and 3.85 ppm (in a 1:1 ratio) are especially diagnostic. The first arises from the two outer benzylic sites of the allyl fragment, while the second is from the two PhCH_2 protons. Therefore, the molecule contains a mirror plane, and we propose a symmetric *endo-endo* arrangement of the phenyl rings, as shown in eq 8.

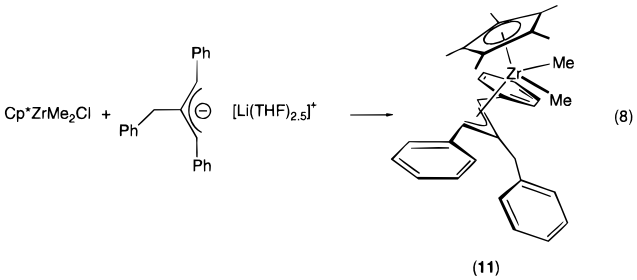

(8)

Methane elimination from **11** is slow and does not proceed as cleanly as is the case of **10**. After 48 h, the major product (approximately 90%) has spectral features in the ^1H NMR spectrum consistent with the formulation [Cp*(TBM)ZrMe-(THF)] (**12**). For **12** there are three phenyl rings which do not interconvert at room temperature. Correspondingly, there are three benzylic hydrogen peaks, one Cp* signal, and a singlet at 0.40 ppm (three hydrogens relative to Cp*) assigned to Zr−Me. A weakly coordinated THF (easily displaced by THF-d_8) was deduced from multiplets at 2.99, 2.63, and 0.88 ppm which integrated to a 2:2:4 ratio. In view of the stereochemistry observed in the product from the reaction of **12** with 2-butyne

(27) Boche, G.; Buckl, K.; Martens, D.; Schneider, D. R. *Liebigs Ann. Chem.* **1980**, 1135.

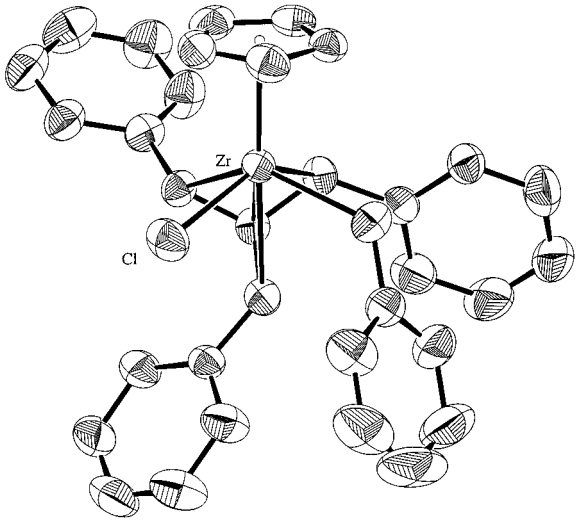

Figure 3. ORTEP diagram of **9**. The Cp* methyls and the countercation are omitted for clarity. Thermal ellipsoids are drawn at the 50% probability level.

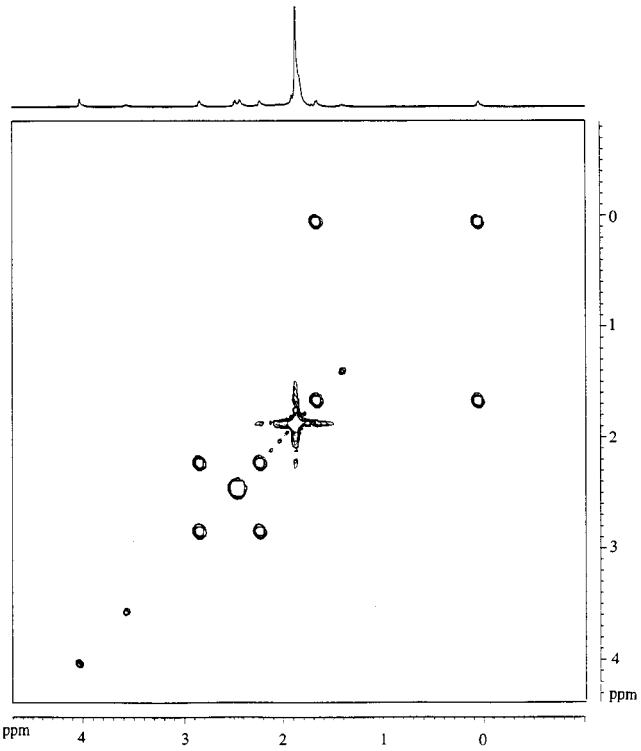

Figure 4. ^1H NMR COSY (C_6D_6) spectrum at 298 K of compound **10**.

(*vide infra*), we propose that the phenyl rings in **12** have the arrangement shown in eq 9. The rates of disappearance of **11**

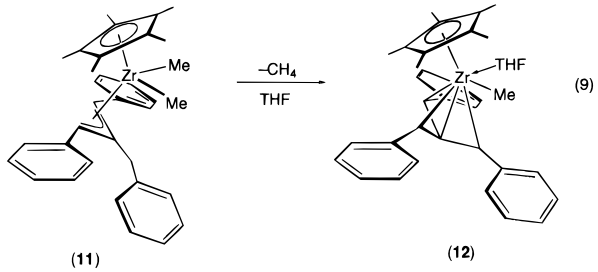

(9)

and appearance of **12** are identical and concentration independent, a good indication that methane elimination is an intramo-

Scheme 3

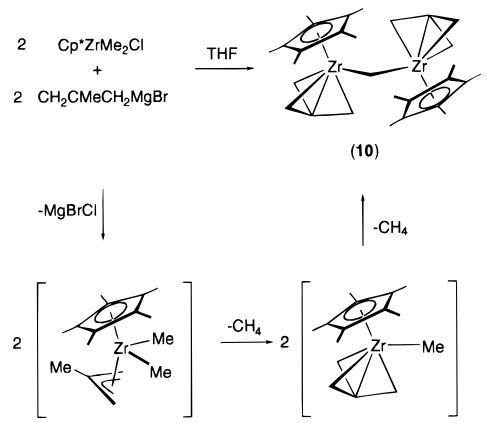

lecular process. Attempts to isolate crystalline samples of **12** were frustrated by impurities and, more importantly, its thermal instability. Partial decomposition of **12** occurs by the time **11** is totally consumed.

A new organometallic species appears when crude **12** is dissolved in neat 2-butyne. This complex contains one Cp*, a TBM ligand with inequivalent benzylidene arms, two diastereotopic hydrogens (quartet, $J_{HH} = 2.5$ Hz, of doublets, $J_{HH} = 11$ Hz), and one methyl (triplet, $J_{HH} = 2.5$ Hz). A low-temperature single-crystal diffraction study revealed the molecular structure shown in Figure 5. The Cp* and η^4-TBM ligands are bound to Zr creating a bent metallocene-like environment. The four-carbon fragment, located roughly in the standard metallocene plane, is readily identifiable as an η^3-propargyl ligand. It is interesting to note that the original orientation of phenyl substituents relative to each other in *endo-endo*-[Li][$PhCH_2C(CHPh)_2$] is retained, *i.e.*, two rings point away from each other, thus defining the alternative, nonsymmetric isomer possible for TBM. Therefore, the reaction of [Cp*(TBM)ZrMe(THF)] with 2-butyne gives Cp*(TBM)Zr(η^3-CH_2CCMe) (**13**) as shown in eq 10.

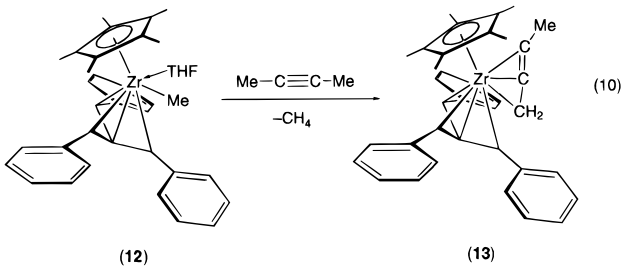

(10)

Careful examination of **13** reveals other important details. The *syn*-bound TBM is rotated so that two phenyl rings point away from the "back" side of the metallocene and avoid the large Cp* ligand. The essentially linear η^3-CH_2CCMe fragment prefers to slide within the metallocene plane to minimize interferences with the phenyl ring. Note how C_{35} is essentially contained in the $Cp^*_{cent}-Zr-C_{11}$ plane, placing C_{34} and C_{33} above the quadrant with less steric interference from TBM (see Figure 5). The Zr−(η^3-CH_2CCMe) distances of $Zr-C_{33} = 2.498(5)$ Å, $Zr-C_{34} = 2.408(4)$ Å, and $Zr-C_{35} = 2.444(5)$ Å coupled with the intraligand metrical parameters of $C_{33}-C_{34}$ (1.376(7) Å), $C_{34}-C_{35}$ (1.218(7) Å), and $C_{35}-C_{36}$ (1.497(7) Å) imply that the best description of the CH_2CCMe fragment is a combination of η^3-propargyl (A) and η^3-allenyl (B) resonance structures.

Polymerization and Copolymerization Activity with Methylaluminoxane. The *in situ* generation of **12** and alkylation of

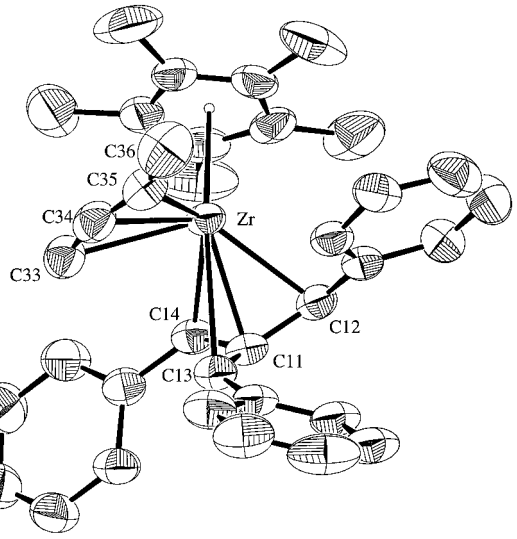

Figure 5. ORTEP diagram of **13**. Thermal ellipsoids are drawn at the 50% probability level.

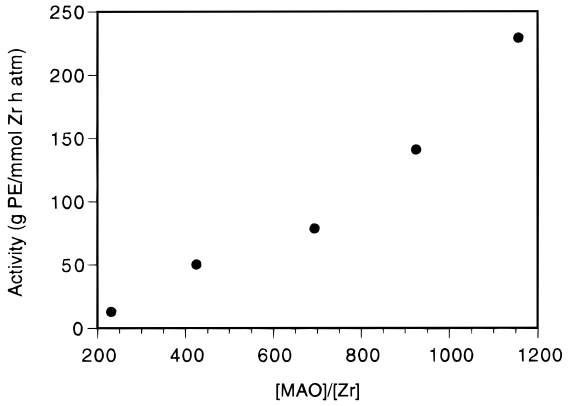

Figure 6. Polymerization activity obtained using **2** and various equivalents of MAO.

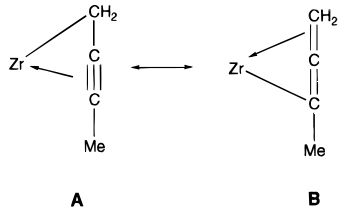

2 to **7** suggested that the combination of complexes **2**−**6** with methylaluminoxane (MAO) could result in the formation of catalytically active *neutral* alkyls.[28] We tested this idea by dissolving a small quantity of zirconium salt (usually 10 mg) into 10 mL of MAO solution (6.4% Al in toluene). After 5−10 min, a constant flow of ethylene (1 atm) at room temperature was passed over the solution under vigorous stirring. In all cases, precipitation of PE, together with generation of heat, was observed. Polymerization activities with **2** as a function of MAO concentration were measured in order to determine the optimum amount of cocatalyst required. Figure 6 shows a nearly linear relationship between polymerization activity and [MAO] in the range of concentrations accessible for these studies. This result is not unusual for metallocenes.[29] An arbitrary amount of MAO (Al:Zr ratio of 800(10)) was chosen for all polymerizations.

We speculate that MAO plays its standard role in these reactions, namely, it alkylates zirconium and removes a ligand

(28) Resconi, L.; Bossi, S.; Abis, L. *Macromolecules* **1990**, *23*, 4489.
(29) Jüngling, S.; Mülhaupt, R. *J. Organomet. Chem.* **1995**, *497*, 27.

Table 2. Ethylene Polymerization Data[a]

catalyst[b]		activity (g of PE/mmol of Zr·atm·min)
Cp*(TMM)$ZrCl_2$Li(TMEDA)	(**1**)	1.7
Cp*(TBM)$ZrCl_2^-$	(**2**)	7.2
Cp(TBM)$ZrCl_2^-$	(**3**)	1.5
Cp*(DBM)$ZrCl_2^-$	(**6**)	1.4

[a] Time = 30 min, 6 mL of MAO for all the reactions (MAO was 6.4 wt % Al in toluene), 10 mg of catalyst. [b] Only the anion is shown for clarity.

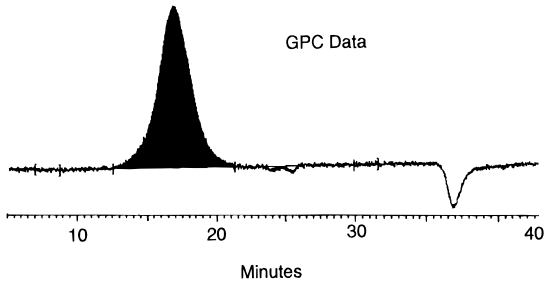

Figure 7. GPC elution curve of polymer produced by **2**.

to create a neutral complex, *i.e.*, "Cp*(TBM)ZrMe" from **2**. To establish the reactivity of a neutral 14-electron species of this type, ethylene was added to a solution containing Cp*(TBM)-ZrMe (prepared in benzene from decomposition of **11**). After a short period of time, PE precipitates out of solution. A quantitative measure of activity could not be obtained as the concentration of Cp*(TBM)ZrMe is time dependent. Qualitatively, the reactivity of Cp*(TBM)ZrMe is similar to that of **2**/MAO. A more specific comparison is further complicated by MAO's ability to remove impurities, *i.e.*, oxygen and moisture, that may be present in ethylene gas.

The amounts of polymer generated using **1**−**3** and **6** are shown in Table 2 (insolubility prevented molecular weight determination by gel permeation chromatography). Although the activities of these catalysts are lower than those of cationic group 4 metallocenes,[6] they are high when compared against isostructural and isoelectronic group 3 metallocenes. Immediately obvious from Table 2 is the better performance of **2** which contains the sterically most demanding ligands. Judging from the stabilities of [Cp*(TBM)ZrMe] versus transient "[Cp*-(TMM)ZrMe]", it is possible to rationalize the activities in Table 2 in terms of bimetallic deactivation reactions. The large Cp* and TBM ligands in **2** discourage approach of two metal centers to each other.

Problems associated with the low solubility of PE homopolymer are often circumvented by incorporating 1-hexene along the PE backbone.[30] More importantly, the preparation of linear low-density polyethylene (LLDPE) *via* the addition of α-olefins during PE formation is a commercially valuable technology.[6c] We measured the ability of different catalyst mixtures to consume 1-hexene under 4 atm of ethylene at 60 °C. The resulting polymers were purified, and the percent content of butyl branches was determined by high-temperature ^{1}H NMR spectroscopy.[31] The results of these studies are presented in Table 3 (monomodal molecular weight distributions were observed by GPC in all cases, see Figure 7). Although the incorporation of 1-hexene is low for all cases, it is interesting to note smaller ligands allow for formation of more branched material.

Cyclopolymerization of 1,5-hexadiene was carried out to probe α-olefin polymerization activity and to determine if the resulting polymer stereochemistry is related to the ligand environment of the metal center (Table 4).[32] These experiments are of great utility in light of the large and excellent body of data available in the literature for determining polymer microstructure by ^{13}C NMR spectroscopy.[6,33] Immediately obvious are the correlations of the cyclopolymerization results between **2** and **3** with Cp*$_2$$ZrCl_2$ and Cp_2ZrCl_2, respectively. The trans content, M_w, and M_n are very similar for these two pairs of precatalysts. It seems that Cp and Cp* not only dominate the gross molecular geometries in the precatalyst but are also responsible for the general reactivity patterns in polymerization reactions.

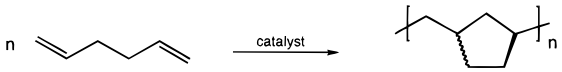

Conclusion

The most general method for coordinating TMM ligands to zirconium involves direct complexation using the dilithium salts of the ligands. This approach is exemplified by eq 2. It is abundantly evident from the series of crystallographic determinations that the "Cp(TBM)Zr" fragment is structurally and electronically similar to "Cp_2Ln" (where Ln = lanthanide or group 3 metal). However, unlike lanthanide chemistry, the formation of discrete salts, *i.e.*, [Cp*(TBM)$ZrCl_2$][Li(TMEDA)$_2$] (**2**), instead of zwitterions predominates. It seems that zirconium prefers to retain both chloride ligands, and therefore the lithium cation must be enclosed within a strongly ligating tetrahedral environment. That Li_2(TBM)(DME)$_2$ (DME = dimethoxyethane) fails as a source of ligand is significant in this respect. DME is a weaker donor than TMEDA and may not be able to prevent LiCl formation.

To prepare neutral d^0, 14-electron alkyls, such as **12**, one must rely on intramolecular methane elimination reactions (eq 9). "Cp*(TMM)ZrMe" is unstable toward formation of the bridging methylene complex **10** (Scheme 3). Incorporation of larger TBM instead of TMM, as in **12**, increases the lifetime of the monomeric species. Most significantly, **12** is a catalyst for ethylene polymerization and can participate in σ-bond metathesis reactions, as shown by the formation of **13** in eq 10.

We have also shown that ethylene polymerization catalysts form when zirconium salts **2**−**6** are treated with MAO. It is most likely that the catalysts are 14-electron alkyls similar to the THF-free version of **12**. Note that the narrow and monomodal molecular weight distribution suggests that only one catalyst species is present in solution. Polymerization data listed in Table 2 provide insight into the structural requirements of neutral catalysts. Best results for ethylene polymerization are obtained with **2** which contains the most crowded ligand environment. This protection discourages bimolecular deactivation processes, such as that shown in Scheme 3. It is interesting to note that in typical metallocene catalysts of general formula [Cp_2ZrMe]$^+$, mutual Coulombic repulsion disfavors bimolecular approach, even when smaller ligands are used.

Experimental Section

General Considerations. All manipulations were carried out using either high-vacuum or glovebox techniques as described previously.[34] ^{1}H and ^{13}C NMR spectra were recorded on a Bruker AMX-400 NMR

(30) (a) Böhm, L. L. *J. Appl. Polym. Sci.* **1984**, *29*, 279. (b) Cozewith, C.; Ver Strate, G. *Macromolecules* **1971**, *4*, 482.

(31) Jaber, I. A.; Fink, G. *J. Mol. Catal. A: Chem.* **1995**, *98*, 135.

(32) Cheng, H. N.; Khasat, N. P. *J. Appl. Polym. Sci.* **1988**, *35*, 825.

(33) (a) Resconi, L.; Coates, G. W.; Mogstad, A.; Waymouth, R. M. *J. Macromol. Sci. − Chem.* **1991**, *A28*, 1225. (b) Coates, G. W.; Waymouth, R. M. *J. Am. Chem. Soc.* **1991**, *113*, 6270. (c) Coates, G. W.; Waymouth, R. M. *J. Am. Chem. Soc.* **1993**, *115*, 91.

(34) Burger, B. J.; Bercaw, J. E. In *Experimental Organometallic Chemistry*; Wayda, A. L., Darensbourg, M. Y., Eds.; ACS Symposium Series 353; American Chemical Society: Washington, DC, 1987.

Table 3. Ethylene−1-Hexene Copolymerization Data[a]

precatalyst	wt of cat. (mg)	time (min)	M_w ($\times 10^{-5}$)	activity (g of PE/mmol·atm·min)	equiv of mol % hexene
Cp*Zr(TMM)Cl_2Li(TMEDA)	18	60	1.4	NM[b]	1.2
Cp*Zr(DBM)Cl_2^-	16	120	1.5	93	1.9
Cp*Zr(TBM)Cl_2^-	15	100	1.5	132	1.6
CpZr(TBM)Cl_2^-	15	60	4.0	34	7.4

[a] Temp = 60 °C; ethylene added = 75 psi; 1-hexene added = 45 mL; MAO = 10 mL (10 wt %). [b] Not measured.

Table 4. Cyclopolymerization of 1,5-Hexadiene[a]

no.	precatalyst	[Al]/[Zr]	conversion	trans (%)[b]	cyclization[c] (%)	M_w[d] ($\times 10^{-3}$)	M_n[d] ($\times 10^{-3}$)	polydispersity[d]
3	Cp(TBM)$ZrCl_2^-$	820	55	75	>99	26	16	1.6
2	Cp*(TBM)$ZrCl_2^-$	850	25	25	>99	3.1	2.0	1.6
6	Cp*(DBM)$ZrCl_2^-$	900	25	23	97	3.3	15	2.4
	Cp*$_2$$ZrCl_2$[34]	1000	65.0	14	>99	3.5	1.5	NR
	Cp_2ZrCl_2[34]	2300	11.1	80	>99	27	13	NR

[a] T = 25 °C. [b] Determined by ^{13}C NMR. [c] Determined by ^{1}H NMR. [d] Determined by GPC versus polystyrene.

Table 5. Summary of Crystallographic Data

	3	**6**	**9**	**13**
empirical formula	$ZrC_{39}H_{55}Cl_2LiN_4$	$ZrC_{38}H_{61}Cl_2LiN_4$	$ZrC_{53}H_{72}ClLiN_2O_2$	$ZrC_{36}H_{38}$
formula weight, amu	748.96	742.99	902.86	561.96
crystal size, mm	0.60 × 0.30 × 0.23	0.15 × 0.38 × 0.23	0.60 × 0.60 0.45	0.60 × 0.48 × 0.50
cryst syst	monoclinic	orthorhombic	monoclinic	triclinic
space group	$P2_1/c$ (No. 14)	*Pbca* (No. 61)	*Cc* (No. 9)	$P\bar{1}$ (No. 2)
Z	4	8	4	2
a, Å	20.0528(3)	14.40(1)	16.590(6)	10.4957(3)
b, Å	19.1933(3)	33.85(2)	19.190(1)	12.8614(4)
c, Å	23.0594(3)	16.882(6)	16.155(8)	14.6535(4)
α, deg	90	90	90	104.635(1)
β, deg	109.088(1)	90	102.67(4)	98.640(2)
γ, deg	90	90	90	111.421(2)
V, Å^3	8387.1(2)	8226(13)	5018(8)	1715.9(1)
d_{calc}, g/cm^3	1.177	1.20	1.20	1.09
T, °C	−60	−60	−60	−50
data collected	$\pm h, \pm k, \pm l$	$h, k, \pm l$	$h, k, \pm l$	$\pm h, \pm k, \pm l$
reflections collected	34289	7125	4729	7087
unique reflections (R_{int})	12494 (0.043)	3737 (0.164)	4602 (0.033)	4852 (0.027)
no. of observations ($I > 3.00s(I)$)	9085	1241	3890	4554
no. of parameters varied	806	305	539	358
abs coeff, cm^{-1}	4.18	4.21	3.06	3.39
abs correction	semiemperical	differential	differential	semiemperical
range of transm factors	0.860−1.01	0.85−1.07	0.78−1.16	0.760−1.01
R;[a] R_w[b]	0.081; 0.101	0.059; 0.068	0.041; 0.048	0.052; 0.079
max shift/error in final cycle	0.24	0.04	0.37	0.08
goodness of fit[c]	4.30	2.21	1.92	4.63
largest peaks in final E map	−0.69; 1.60	−0.49; 0.51	−0.31; 0.43	−0.66; 0.69

[a] $R = \sum(|F_o| - |F_c|)/\sum|F_o|$. [b] $R_w = [\sum_w(|F_o| - |F_c|)^2/\sum_w|F_o|^2]^{1/2}$. [c] S = goodness of fit = $(\sum(|F_o| - |F_c|)/\sigma]/(n - m)$, where n is the number of reflections used in the refinement and m is the number of variables.

spectrometer at 400.1 and 100.6 MHz, respectively. Toluene, pentane, diethyl ether, and tetrahydrofuran were distilled from benzophenone ketyl. Elemental analyses were carried out by Desert Analytics. The preparations of Li_2(TBM)(TMEDA)$_2$,[21] Li_2(TMM)(TMEDA)$_2$,[35] Li_2-(DBM)(TMEDA)$_2$,[13] Cp*$ZrCl_3$,[22] Cp*$ZrMe_3$,[22] Cp*$ZrCl_2(CH_2Ph)$,[22] and $CpZrCl_3$(DME)[36] are available in the literature. MAO was purchased from AKZO Chemicals (toluene, 6.4 wt % Al, type 4). Nitrogen analyses were consistently low, even after repeated attempts. We suspect that formation of lithium nitride results in lower nitrogen values. Carbon and hydrogen analyses, however, were acceptable. Crystallographic details can be found in the Supporting Information.

2-Benzyl-1,3-diphenyl-1-propene. This is a modification of the procedure described in the literature.[25] A diethyl ether solution (200 mL) of 1,3-diphenylacetone (25 g, 0.088 mol) was slowly added to $PhCH_2MgCl$ (1.0 M in diethyl ether, 88.0 mL). Toward the end of the addition a white precipitate was observed. After 12 h, the reaction vessel was immersed in an ice bath (0 °C), the reaction quenched with 300 mL of 5% H_2SO_4, and the mixture stirred for 1 h. The organic layer was separated, washed twice with brine (2 × 100 mL), and dried over $MgSO_4$. Decanting of the filtrate followed by solvent evaporation afforded tribenzylcarbinol (Bz_3COH) as a white crystalline material in 85% yield. The alcohol was dissolved in 200 mL of glacial acetic acid containing a catalytic amount of concentrated H_2SO_4 (10 drops) and refluxed for 4 h. The reaction mixture was then chilled, and 200 mL of water and 300 mL of Et_2O were added. The organic layer was washed with 0.5 M NaOH until basic. The preparation of the diphenyl analog is similar with the exception that MeMgCl is used instead of the $PhCH_2MgCl$.[13]

Li_2(DBM)(TMEDA)$_2$,[13] **Li_2('TBM)(TMEDA)$_2$, and Li_2(TBM)-(TMEDA)$_2$.**[35] The appropriate olefin was dissolved in pentane and 2.1 equiv of a 1:1 mixture of *n*-BuLi:TMEDA in hexane is added dropwise. After stirring for 12 h, the deep red dianion was filtered, washed with a minimum amount of cold pentane, and dried under vacuum. Typical yields are within 60−70%. These salts are extremely thermally and air sensitive and are best stored at −30 °C in a nitrogen atmosphere.

Li(PhCH)$_2$CCH$_2$Ph(THF)$_{2.5}$. This is a modification of a previously described procedure. A THF solution of LDA was added slowly to 2-benzyl-1,3-diphenyl-1-propene to afford a red solution which was

(35) Jones, M. D.; Kemmett, R. D. W. *Adv. Organomet. Chem.* **1987**, *27*, 279.
(36) Lund, E.; Livinghouse, T. *Organometallics* **1990**, *9*, 2426.

stirred overnight. The solvent was replaced with pentane and stirred for 3 days to give an orange solid which was collected by filtration and washed twice with a minimum amount of cold pentane. Spectroscopic data are consistent with previous characterization: ^{1}H NMR (C_6D_6) δ 7.68−6.69 (m, 15H, $-C_6H_5$), 5.27 (s, 2H, (PhC*H*)$_2$C), 4.01 (s, 2H, CH_2Ph), 3.12 (t, 10H, OCH_2), 1.15 (m, 10H, OCH$_2$CH_2).

[Cp*(TBM)ZrCl$_2$][Li(TMEDA)$_2$] (2). A toluene solution of Li$_2$TBM(TMEDA)$_2$ (0.529 g, 1.00 mmol) was added to a toluene suspension of Cp*ZrCl$_3$ (0.333 g, 1.00 mmol) and stirred for 3 h. Evaporation was followed by a diethyl ether extraction. Solvent removal and a pentane wash provided the product as a red solid in 71% yield (0.580 g): ^{1}H NMR (C_6D_6, 25 °C) δ 1.90 (C_5Me_5), 2.06 (s, 8, Me$_2$NCH_2CH_2NMe$_2$), 2.09 (s, 24, *Me*$_2$NCH$_2$CH$_2$N*Me*$_2$), 6.55 (t, 3, *p*-*H*-C$_6$H$_5$), 7.03 (t, 6, *m*-*H*-C$_6$H$_5$), 7.51 (b, 6, *o*-*H*-C$_6$H$_5$), C(C*H*-C$_5$H$_6$)$_3$ signals not observed (likely to be broadened into the baseline); ^{1}H NMR ($C_6D_5CD_3$, −30 °C) δ 3.40, 3.58, 4.16 (s, 1, C(C*H*-C$_6$H$_5$)$_3$, ea); ^{13}C NMR (THF-d_8) δ 141.5 (*C*(CH-C$_6$H$_5$)$_3$), 129.0 (*m*-C(CH-*C*$_6$H$_5$)$_3$), 128.4 (*o*-C(CH-*C*$_6$H$_5$)$_3$), 127.3 (*p*-C(CH-*C*$_6$H$_6$)$_3$), 120.9 (C(*C*H-C$_6$H$_6$)$_3$), 120.3 (*C*$_5$Me$_5$), 58.9 (Me$_2$N*C*H$_2$CH$_2$NMe$_2$), 46.2 (*Me*$_2$NCH$_2$CH$_2$N*Me*$_2$), 12.3 (C$_5$*Me*$_5$), *ipso* carbons in the TBM ligand not observed. Anal. Calcd for ZrC$_{44}$H$_{65}$Cl$_2$LiN$_2$: C, 64.45; H, 7.99; N, 6.85. Found: C, 64.07; H, 7.52; N, 5.77.

[Cp(TBM)ZrCl$_2$][Li(TMEDA)$_2$] (3). A toluene solution of Li$_2$TBM(TMEDA)$_2$ (0.679 g, 1.28 mmol) was added dropwise to a toluene suspension of CpZrCl$_3$·DME (0.453 g, 1.28 mmol) and stirred for 3 h. After solvent removal, the residue was heated to 60 °C for 1 h while under dynamic vacuum. A brick-red solid was left from which the product was extracted with copious amounts of a 1:1 dimethyl ether: benzene mixture. Solvent evaporation, followed by pentane wash, and filtration afforded the product as a solid in 46% yield (0.445 g). Analytically pure crystals can be obtained from slow evaporation of a diethyl ether solution: ^{1}H NMR (C_6D_6: THF-d_8, 1:1) δ 7.50 (b, 6H, *o*-Ph), 7.09 (t, 6H, *m*-Ph), 6.78 (t, 3H, *p*-Ph), 6.25 (s, 5H, C$_5$*H*$_5$), 2.12 (s, 8H, NCH_2), 2.06 (s, 24H, NCH_3), PhC*H* signals broad and centered at 4.74 ppm; ^{13}C NMR (C_6D_6: THF-d_8, 1:1) δ 139.5 ((PhCH)$_3$*C*), 129.2, 127.6, 125.6, 121.2 (C$_6$H$_5$CH), 114.5 (*C*$_5$H$_5$), 57.5 (N*C*H$_2$), 46.0 (N*C*H$_3$). Anal. Calcd for ZrC$_{39}$H$_{55}$Cl$_2$LiN$_4$: C, 62.54; H, 7.42; N, 7.48. Found: C, 62.30; H, 7.21; N, 6.76.

[Cp(*t*-Bu-TBM)ZrCl$_2$][Li(TMEDA)$_2$] (4). To a stirring solution of CpZrCl$_3$·DME (0.398 g, 1.13 mmol) in THF was added dropwise a solution of [*t*-Bu-TBM][Li(TMEDA)$_2$] (0.659 g, 1.13 mmol) in THF. After 1 h the solvent was removed and the product extracted with a diethyl ether:methylene chloride solvent mixture (1:1). The volume of the solution was reduced by one-half and pentane added. Cooling this solution for 1 h at −30 °C afforded the product as a red-orange semisolid (62%, 0.560 g): ^{1}H NMR (THF-d_8) δ 7.33−6.85 (m, 12H, *o*-Ph, *m*-Ph), 6.65 (t, 3H, *p*-Ph), 5.98 (s, 5H, C$_5$*H*$_5$), 4.34 (bs, 3H, C(C*H*Ph)$_3$), 2.30 (s, 8H, NCH_2), 2.15 (s, 24H, NCH_3), 1.27 (s, 9H, C(CH_3)$_3$); ^{13}C NMR (THF-d_8) δ 143.0 (*C*(CHPh)$_3$), 139.3, 128.0, 126.5, 124.8, 123.3, 121.5, 120.0, 114.9 (C(CH*C*$_6$H$_5$)), 113.2 (*C*$_5$H$_5$), 58.5 (N*C*H$_2$), 45.8 (N*C*H$_3$), 33.4 (*C*(CH$_3$)$_3$), 31.7 (C(*C*H$_3$)$_3$). The oily nature of this compound prevented accurate elemental analysis.

[Cp*(*t*-Bu-TBM)ZrCl$_2$][Li(TMEDA)$_2$] (5). To a stirring THF solution of Cp*ZrCl$_3$ (0.378 g, 1.14 mmol) was added dropwise a THF solution of [*t*-Bu-TBM][Li(TMEDA)$_2$] (0.664 g, 1.14 mmol). After 1 h the solvent was removed *in vacuo* and the product extracted with diethyl ether. Solvent removal and extensive trituration with pentane afforded the product as a red-orange semisolid in 60% yield (0.60 g). Small quantities of analytically pure material can be obtained from recrystallization in pentane at −30 °C: ^{1}H NMR (CDCl$_3$) δ 7.28−7.07 (m, 12H, *o*-Ph, *m*-Ph), 6.18 (t, 2H, *p*-Ph), 4.61 (s, 3H, C[C*H*Ph]), 2.31 (s, 8H, NCH_2), 2.18 (s, 24H, NCH_3), 1.75 (s, 15H, C$_5$(CH_3)$_5$), 1.24 (s, 9H, C(CH_3)$_3$); ^{13}C NMR (CDCl$_3$) δ 145.8 (*C*(CHPh)$_3$), 130.4−124.2 (C(CH*C*$_6$H$_5$)), 121.6 (*C*$_5$(CH$_3$)$_5$), 56.9 (N*C*H$_2$), 46.0 (N*C*H$_3$), 31.5 (*C*(CH$_3$)$_3$), 31.0 (C(*C*H$_3$)$_3$), 11.8 (C$_5$(*C*H$_3$)$_5$). Anal. Calcd for ZrC$_{48}$H$_{73}$Cl$_2$LiN$_4$: C, 65.86; H, 8.42; N, 6.40. Found: C, 65.49; H, 7.60; N, 4.50.

[Cp*(DBM)ZrCl$_2$][Li(TMEDA)$_2$] (6). A stirring solution of Cp*ZrCl$_3$ (0.300 g, 0.90 mmol) in benzene was treated dropwise with a solution of Li$_2$DBM(TMEDA)$_2$ (0.410 g, 0.90 mmol) in benzene. After stirring for 3 h the solvent was replaced with diethyl ether and filtered in order to remove LiCl. The ether was removed and the residue washed with pentane to provide a brick-red solid (57%, 0.381 g). Crystals for X-ray and elemental analyses can be obtained by slow evaporation of a concentrated benzene solution: ^{1}H NMR (THF-d_8) δ 7.58−6.78 (m, 10H, C$_6$*H*$_5$), 2.11 (s, 8H, NCH_2), 2.07 (s, 15H, C$_5$(CH_3)$_5$), 1.99 (s, 24H, NCH_3); ^{13}C NMR (THF-d_8) δ 146.8, 129.4−120.3 (CH$_2$C-(CH*C*$_6$H$_5$)$_2$), 57.7 (N*C*H$_2$), 45.8 (N*C*H$_3$), 12.52 (C$_5$(*C*H$_3$)$_5$). The TMM inner core protons and carbons were broadened into the baseline due to fast rotation on the NMR time scale. Anal. Calcd for ZrC$_{38}$H$_{60}$-Cl$_2$LiN$_4$: C, 61.50; H, 8.17; N, 7.55. Found: C, 61.78; H, 8.19; N, 5.89.

[Cp*(TBM)ZrCl(CH$_2$Ph)][Li(TMEDA)$_2$] (9). Li$_2$TBM(TMEDA)$_2$ (0.400 g, 0.78 mmol) in toluene was added to a stirring solution of Cp*ZrCl$_2$(CH$_2$Ph) (0.395 g, 0.78 mmol) in toluene, and the mixture was stirred for 3 h. The resulting solids (most likely LiCl) were filtered, the volume was reduced by approximately 80%, and pentane was added to induce further precipitation. This slurry was cooled overnight and the product collected by filtration as an orange microcrystalline solid (88%). Crystallization for further (X-ray and elemental) analyses was carried out in a mixture of CH$_2$Cl$_2$ with small amounts of THF. One TMEDA of the [Li(TMEDA)$_2$] countercation was displaced by two THF's during crystallization (determined by ^{1}H NMR, elemental analysis, and X-ray crystallography): ^{1}H NMR (THF-d_8) δ 7.20−6.61 (20H, Ph), 2.24 (d, 1H, CH_2Ph, $J_{H-H'}$ = 9.84 Hz), 2.25 (s, 8H, NCH_2), 2.50 (s, 15H, C$_5$(CH_3)$_5$), 1.97 (s, 24H, NCH_3), 0.96 (d, 1H, CH_2Ph, $J_{H-H'}$ = 9.84 Hz); ^{13}C NMR (C_6D_6: THF-d_8, 1:1) δ 158.3 (*C*(CHC$_6$H$_5$), 139.2−119.4 (C(CH*C*$_6$H$_5$), 118.1 (*C*$_5$(CH$_3$)$_5$), 57.9 (N*C*H$_2$), 45.9 (N*C*H$_3$), 43.6 (Zr-CH$_2$Ph), 12.4 (C$_5$(*C*H$_3$)$_5$). Anal. Calcd for ZrC$_{53}$-H$_{72}$ClLiN$_2$O$_2$: C, 71.06; H, 8.05; N, 3.10. Found: C, 71.12; H, 8.09; N, 5.17.

[Cp*(TMM)Zr]$_2$(μ-CH$_2$) (10). A THF solution of Cp*Zr(CH$_3$)$_2$-Cl (0.445 g, 1.52 mmol) at −30 °C was treated with 2.37 mL of (2-methylallyl)magnesium bromide (0.64 M in THF) and stirred for 30 min. The solvent was replaced with benzene and the reaction mixture filtered. Benzene evaporation provided the product as a red solid which may be washed with pentane in order to remove any remaining impurities. Recrystallization from pentane afforded analytically pure red plates: ^{1}H NMR (C_6D_6) δ 4.02 (s, μ-CH_2), 2.83, 2.49, 2.42, 2.21, 1.68, 0.05 (d, (CH_2)$_3$C), 1.88 (s, 15H, C$_5$(CH_3)$_5$); ^{13}C NMR (C_6D_6, J_{C-H} in Hz) δ 180.1 (s, (CH$_2$)$_3$*C*), 146.5 (t, Zr*C*H$_2$Zr, J_{C-H} = 115.7), 117.9 (s, *C*$_5$(CH$_3$)$_5$), 77.3 (t, (*C*H$_2$)$_2$CCH$_2$···Zr, J_{C-H} = 152.6), 66.0 (t, (*C*H$_2$)$_2$-CCH, J_{C-H} = 152.6), 62.4 ((CH$_2$)$_2$*C*CH$_2$···Zr, J_{C-H} = 127.2), 12.3 (q, C$_5$(*C*H$_3$)$_5$, J_{C-H} = 125.9). Anal. Calcd for ZrC$_{29}$H$_{44}$: C, 60.55; H, 7.73. Found: C, 60.64; H, 7.78.

Cp*Zr(CH$_3$)$_2$((PhCH)$_2$CCH$_2$Ph) (11). Cp*Zr(CH$_3$)$_2$Cl (0.300 g, 1.03 mmol) was dissolved in benzene and treated with Li(PhCH)CCH$_2$-Ph(THF)$_{2.5}$ (0.484 g, 1.03 mmol). After stirring for 10 min, the mixture was filtered and the solvent evaporated to provide the product as a red microcrystalline solid in 63% yield (0.340 g). ^{1}H NMR analysis of the product showed partial decomposition to Cp*(TBM)ZrMe within minutes of preparation: ^{1}H NMR (C_6D_6) δ 7.28−6.91 (aromatic H's), 4.54 (s, 2H, PhC*H*), 3.85 (s, 2H, PhCH_2), 1.62 (s, 15H, C$_5$(CH_3)$_5$), 0.17 (s, 6H, ZrCH_3); ^{13}C NMR (C_6D_6) δ 139.7−118.7 (aromatic C's), 98.6 (*C*$_5$(CH$_3$)$_5$), 78.1 (Ph-*C*H), 44.6 (Zr*C*H$_3$), 25.0 (Ph*C*H$_2$), 11.5 (C$_5$-(*C*H$_3$)$_5$). The thermal instability of this allylic compound prevented elemental analysis (see text).

Cp*(TBM)ZrCH$_3$ (12). This compound was prepared and used *in situ* from the decomposition of **11** in benzene over 2 days. The coordinated THF-d_8 is displaced when THF-d_8 was added to the NMR tube in order to solubilize the product: ^{1}H NMR (C_6D_6/THF-d_8) δ 7.59, 7.11, 6.74 (m, 15H, [C$_6$*H*$_5$CH]$_3$C), 4.71 (b, 3H, [C$_6$H$_5$C*H*]$_3$C), 1.95 (s, 15H, C$_5$(CH_3)$_5$), −0.31 (s, 3H, Zr-CH_3); ^{13}C NMR (C_6D_6/THF-d_8) δ 145.3 (PhCH)$_3$*C*), 129.8−127.6 ((*C*$_6$H$_5$CH)$_3$C), 120.5 (*C*$_5$(CH$_3$)$_5$), 101.5, 83.7, 71.5 ((Ph*C*H)$_3$C), 34.4 (Zr-*C*H$_3$), 11.5 (C$_5$(*C*H$_3$)$_5$). The thermal instability of this compound prevented elemental analysis (see text).

Cp*(TBM)Zr(η^3-CH$_2$C≡CCH$_3$) (13). Material from the previous procedure (0.121 g, 0.23 mmol) was dissolved in a minimum amount of 2-butyne and allowed to stand overnight. The 2-butyne was then removed under reduced pressure and the remaining orange solid washed with cold pentane. These solids were dissolved in a minimum amount of toluene, and pentane was allowed to diffuse slowly at −30 °C. After 20 h, 30 mg of crystalline product was collected. A second crop was obtained by further cooling the mother liquor with further pentane

diffusion (20 mg). The overall yield can be as high as 54% (70 mg): ^{1}H NMR (C_6D_6) δ 7. (d, 2H, Ph), 7.67−6.67 (m, 13H, Ph), 4.25 (s, 1H, (PhC*H*)$_3$C), 3.97 (s, 1H, (PhC*H*)$_3$C), 3.70 (s, 1H, (PhC*H*)$_3$C), 2.51 (dd, $J_{H\text{-}Me}$ = 2.5 Hz, $J_{H\text{-}H'}$ = Hz, 1H, Zr−C*H*$_2$C≡CCH$_3$), 2.30 (dd, 1H, $J_{H\text{-}Me}$ = 2.5 Hz, $J_{H\text{-}H'}$ = Hz, Zr−C*H*$_2$C≡CCH$_3$), 2.01 (t, 3H, Zr−CH$_2$C≡CC*H*$_3$), 1.38 (s, 15H, C$_5$(C*H*$_3$)$_5$)); ^{13}C NMR (C_6D_6) δ 146.7 ((PhCH)$_3$*C*), 135.1−123.1 ((*C*$_6$H$_5$CH)$_3$C), 114.2 (*C*$_5$(CH$_3$)$_5$), 99.9, 91.7 (Zr−CH$_2$*C*≡*C*H$_3$), 91.7, 83.2, 78.1 ((Ph*C*H)$_3$C), 51.0 (Zr−*C*H$_2$C≡CCH$_3$), 11.2 (C$_5$(*C*H$_3$)$_5$), 11.0 (Zr−CH$_2$C≡C*C*H$_3$). Loss of the toluene of recrystallization renders (see crystallographic section) elemental analyses attempted unreliable. Anal. Calcd for $ZrC_{36}H_{38}$: C, 76.94; H, 6.83. Found: C, 75.44; H, 7.32.

Ethylene Polymerization. This procedure is our own adaptation of standard ethylene polymerizations.[6] Herein is a description of a typical procedure. A small quantity of the catalyst precursor, typically 5−10 mg, was dissolved into a toluene solution containing MAO and allowed to stand for 5−10 min. The reaction flask was then evacuated and filled with 1 atm of ethylene gas. After the appropriate time the reaction was quenched with 10 mL of a 10% HCl methanolic solution. After this mixture stirred for 10 h, the solid PE was filtered, washed four times with methanol, and dried to constant weight.

1,5-Hexadiene Polymerization.[31,32] The catalyst activation is similar as above; however, the monomer (1.00 g, 12.2 mmol) was added dropwise and the resulting mixture stirred for 12 h. The polymerization was quenched with 10 mL of a 10% HCl methanolic solution, volatiles were removed, and the remaining residue was washed with methanol and decanted. The polymer was extracted with 20 mL of $CHCl_3$ and precipitated into acetone. The resulting white solids were filtered, dried to constant weight, and analyzed by ^{1}H NMR, ^{13}C NMR, and GPC.

Ethylene−Hexene Copolymerization. The catalyst mixture was prepared by dissolving the appropriate catalyst precursor (10 mg) in a toluene/MAO solution (8 wt % Al). This mixture was added to a 2 L stainless steel batch reactor containing 400 mL of hexane at 60 °C. The reactor was then charged with 40 mL of 1-hexene and subsequently pressurized with ethylene to 60 psi. The reaction was quenched by exposure to air.

Acknowledgment. We are grateful to Exxon Chemical Co. and the Petroleum Research Fund of the American Chemical Society for financial support of this work. We also thank Dr. R. A. Fisher and Dr. Howard Turner for helpful discussions and the high-temperature polymerization measurements.

Supporting Information Available: Complete crystallographic studies for complexes **3**, **6**, **9**, and **13** (94 pages). See any current masthead page for ordering and Internet access instructions.

JA962545S